PROCEEDINGS OF SCIENCE

Low Momentum Direct Photons in Au+Au collisions at 39 GeV and 62.4 GeV measured by the PHENIX Experiment at RHIC

Vladimir Khachatryan for the PHENIX Collaboration
Department of Physics and Astronomy, Stony Brook University, Stony Brook, NY 11794, USA
E-mail: vladimir.khachatryan@stonybrook.edu

PHENIX has measured low momentum direct photons at 200 GeV via their external conversions to di-electron pairs on a specific detector material. The advantage of this method along with the selection of this detector material is a purity to large extent in photon identification. We present the results of the measurements of low momentum direct photons at 39 GeV and 62.4 GeV based on the same external conversion method. These results, together with those obtained at 200 GeV, can help in constraining the sources of low momentum direct photons. Besides, we report on the observed scaling behavior of direct photons in terms of the photon integrated yield vs. charged-particle multiplicity by combining the data from various collision systems at four center-of-mass energies. The direct photon scaling properties show that the strength of the thermal radiation source grows faster than the charged-particle multiplicity.

CPOD 2017: Critical Point and Onset of Deconfinement
August 7 - 11, 2017
Stony Brook, New York, USA

PoS(CPOD2017)079

1. Introduction

Direct photons, produced during all stages of relativistic heavy ion collisions, are a unique observable to study the fundamental properties of the hot and dense medium produced in these collisions, and can probe the entire space-time evolution of this medium. These photons are defined to be all the produced photons except those that originate from hadronic decays. Being produced from almost all known or conjectured phases after a collision, they have long mean free path and escape the collision region basically unmodified with almost no final state interaction. Thereby, the direct photons carry information on the conditions of their production environment at the time when they are produced. In particular, hard (prompt) direct photons, produced in the preequilibrium phase at high-p_T from initial hard scatterings of incoming partons, carry information on parton distributions in colliding nuclei. Thermal direct photons, produced in and after the equilibrium phase at low-p_T from the Quark Gluon Plasma and Hadronic Gas, provide information about the energy density, temperature and collective motion (azimuthal anisotropy) of the matter. There are also direct photons originating from jet-plasma interactions.

Generally there are three methods for measuring direct photons. These measurement techniques include measuring i) photons that directly deposit energy into electromagnetic calorimeters (EMCals); ii) virtual photons that internally convert into e^+e^- pairs allowing a clean low- or high-p_T measurement; iii) real photons that externally convert into e^+e^- pairs in a well-selected detector material, which also allows a clean low- or high-p_T measurement. The main challenge is usually related to the measurements with the electromagnetic calorimeters, based on the presence of minimal ionizing particles, a large background of photons from final state hadronic decays, and worsening calorimeter resolution. Although all kind of direct photon measurements are challenging especially in the low-p_T region.

Nonetheless, in the low-p_T region, the PHENIX, STAR and ALICE experimental collaborations have observed the thermal yield from Au+Au [1, 2, 3, 4] at RHIC $\sqrt{s_{NN}} = 200$ GeV and from Pb+Pb collisions [5] at LHC $\sqrt{s_{NN}} = 2760$ GeV center-of-mass energies.

2. Measurement details of low momentum direct photons at 39 GeV and 62.4 GeV

Our measurements are based on the external conversion method used for measuring low momentum direct photons in Au+Au at $\sqrt{s_{NN}}$ = 200 GeV [3].

We have analyzed two data samples of 2.12×10^8 (at $\sqrt{s_{NN}}$ = 62.4 GeV) and 7.79×10^7 (at $\sqrt{s_{NN}}$ = 39 GeV) minimum bias Au+Au collisions, which the PHENIX central arm spectrometers have recored in 2010. The final results with the best statistics at 62.4 GeV are obtained for three centrality classes: 0%-20% for the most central selection, 20%-40%, and 0%-86% for minimum bias selection. The results with the best statistics at 39 GeV are obtained for 0%-86% minimum bias selection. The event centrality is categorized by utilizing the PHENIX beam-beam counters (BBCs), which are located down the beam line at 144 cm in both beam directions, covering the pseudorapidity range of $3.1 < |\eta| < 3.9$ and 2π in azimuth.

We measure the raw inclusive photon yield, $N_\gamma^{\rm incl}$, through photon conversions to e^+e^- pairs at well-defined locations in the PHENIX detector, which are in the backplane (consisted of the readout boards and electronics) of the subsystem called Hadron Blind Detector (HBD). The HBD

sits at a radius of 60 cm from the true event vertex. In PHENIX there are two procedures for e^+ and e^- momentum reconstruction. The first one is the standard PHENIX momentum reconstruction algorithm, which assumes that the charged tracks originate from the true event vertex. In this case the momenta of the conversion candidates are initially mismeasured, by which the pairs acquire an artificial opening angle and are reconstructed with a fake mass (at about $M_{\rm vtx} \approx 12\,{\rm MeV}/c^2$), by having the vertex as the tracks' origin. However, in the second procedure with the Alternate Track Model (ATM), one can recalculate the momenta of the conversion candidates assuming that the conversions occur at the HBD backplane. In this case the e^+e^- pair mass is reconstructed correctly with $M_{\rm HBD} < 4.5$ MeV$/c^2$, consistent with the experimental resolution. The identification of the conversion photons is very accurate because the HBD backplane has a relatively large distance from the event vertex without any comparable radiating material nearby, and has a thickness (in terms of the radiation length) equal to $X/X_0 \approx 2.5 \div 3\%$. In Fig. (1) one can see the 2d reconstructions of the pair mass with the ATM and with the standard PHENIX momentum reconstruction algorithm. The red blob around $(M_{vtx}, M_{HBD}) = (0.012, 0.002)$ GeV/c^2 is the place which the best conversion candidates "occupy". The visible tail reflects very small number of pairs, close to 1%, coming from the Dalitz decays, $\pi^0 \to \gamma e^+ e^-$, and from conversions before the HBD backplane at other radii.

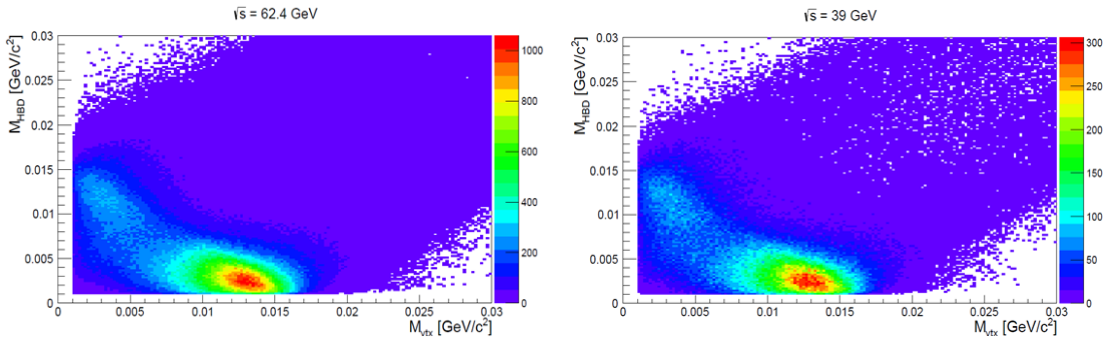

Figure 1: 2d mass plots for a view of the cut space used for the conversion photon identification at $\sqrt{s_{NN}}$ = 62.4 GeV (left panel) and at $\sqrt{s_{NN}}$ = 39 GeV (right panel).

In the analysis we use the following subsystems of the PHENIX detector: drift chambers (DCs) and pad chambers (PCs), whereby the trajectories and momenta of e^+e^- pairs are determined; the pairs are identified by means of the ring-imaging Čerenkov detector (RICH) by requiring a minimum of three RICH phototubes be associated with both charged tracks at the expected ring radius in the interval of 3.4 cm $< r <$ 8.4 cm; the energy of the pairs is measured in the EMCal by requiring that the energy/momentum ratio is greater than 0.5, which means that at least half of the energy expected from tracks should be recovered in the EMCal. The measurements are accomplished down to the converted photon p_T^{ee} equal to 0.5 GeV$/c$. We also measure the π^0 yield for which we pair the inclusive photons reconstructed from conversions with a second photon-like shower reconstructed in the EMCal. A subset of the $N_\gamma^{\rm incl}$ sample is tagged statistically as photons from π^0 decays if they reconstruct the mass of π^0 with these second photons from the EMCal. This is done in bins of p_T^{ee}, not in p_T bins of π^0 . In each p_T^{ee} bin the number of π^0 tagged photons, $N^{\pi^0,{\rm tag}}$, is determined by integrating the $e^+e^-\gamma$ mass distribution around the π^0 mass peak, after subtracting the mixed-event combinatorial background from the di-photon foreground (see Fig. (2)).

In a given p_T^{ee} bin the real yields of inclusive photons, γ^{incl}, and photons from π^0 decays, γ^{π^0}, are related to the experimentally measured quantities N_γ^{incl} and $N^{\pi^0,\text{tag}}$ via

$$N_\gamma^{\text{incl}} = \varepsilon_{ee} a_{ee}\, c\, \gamma^{\text{incl}}, \qquad N^{\pi^0,\text{tag}} = \varepsilon_{ee} a_{ee}\, c\, \langle \varepsilon_\gamma f \rangle \gamma^{\pi^0}, \tag{2.1}$$

where a_{ee} is the pair geometrical acceptance, ε_{ee} is the pair reconstruction efficiency, and c is the probability that a photon conversion happens in the HBD backplane. The product $\langle \varepsilon_\gamma f \rangle$ is the efficiency and acceptance correction for pion tagging, which quantifies the efficiency with which we successfully tag a conversion pair coming from a π^0 decay, given that conversion pair is already reconstructed. The acceptance, efficiency and probability factors explicitly cancel each other in the

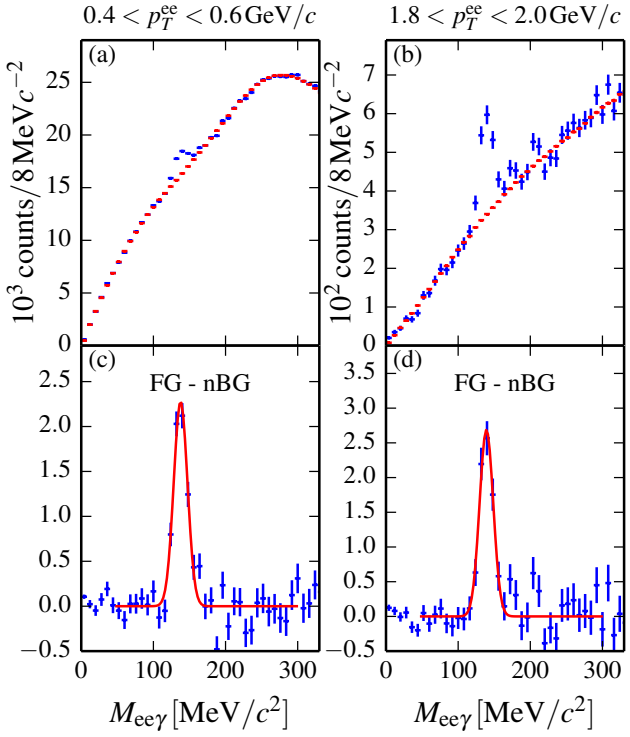

Figure 2: Examples of histograms of the $e^+e^-\gamma$ invariant mass distribution for two different p_T^{ee} bins at $\sqrt{s_{NN}}$ = 200 GeV from [3]. The top plots show the di-photon foreground distribution in blue and normalized combinatorial mixed event background distribution in red. The bottom plots show the isolated pion peak after subtraction of the normalized background from the foreground.

ratio of $N_\gamma^{\text{incl}}/N^{\pi^0,\text{tag}}$. Then we can address R_γ, which is the ratio of γ^{incl} to the real yield of photons from hadronic decays, γ^{hadron}:

$$R_\gamma = \frac{\gamma^{\text{incl}}}{\gamma^{\text{hadron}}} = \frac{\langle \varepsilon_\gamma f \rangle \left(N_\gamma^{\text{incl}}/N_\gamma^{\pi^0,\text{tag}} \right)_{\text{Data}}}{\left(\gamma^{\text{hadron}}/\gamma^{\pi^0} \right)_{\text{Sim}}}. \tag{2.2}$$

In Eq. (2.2) all terms are a function of the converted photon p_T^{ee}. We get the ratio $N_\gamma^{\text{incl}}/N^{\pi^0,\text{tag}}$ in the numerator of Eq. (2.2) from the data analysis, $\langle \varepsilon_\gamma f \rangle$ and the ratio in the denominator from Monte Carlo simulations. R_γ is larger than unity for a given p_T^{ee} if the data sample shows a direct photon signal, however, it is unity if all the photons are hadronic decay products.

3. The PHENIX preliminary results on low momentum direct photons at the two low energies

In Fig. (3) and Fig. (4) we show the results for R_γ in the transverse momentum range of 0.4 GeV/c $< p_T <$ 3.0 GeV/c, and in the centrality bins of 0-20%, 20-40% and minimum bias 0-86% at $\sqrt{s_{NN}}$ = 62.4 GeV as well as in the minimum bias 0-86% at $\sqrt{s_{NN}}$ = 39 GeV. We observe that the data samples at both beam energies show signal of direct photons for the most of 62.4 GeV p_T points, and at least for the lowest p_T points at 39 GeV. Thereby, we can transform these R_γ

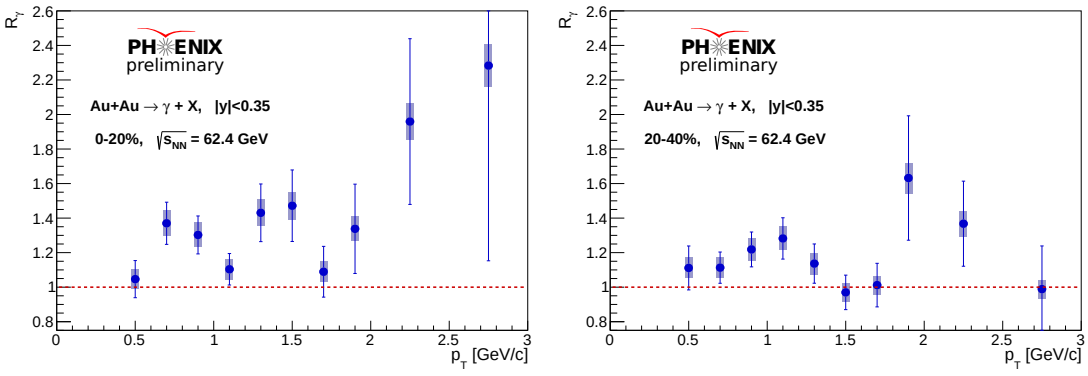

Figure 3: R_γ at $\sqrt{s_{NN}}$ = 62.4 GeV in the centrality bins of 0-20% and 20-40%. The statistical errors are the vertical lines, the systematic errors are the boxes.

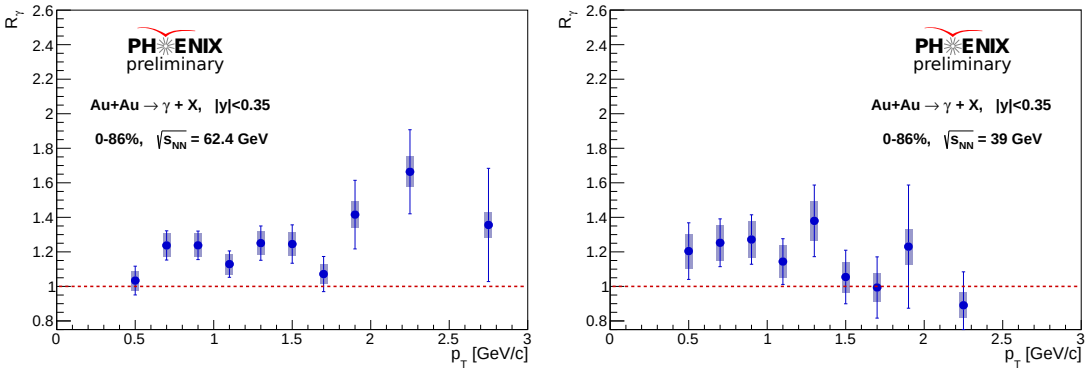

Figure 4: R_γ at $\sqrt{s_{NN}}$ = 62.4 GeV in the minimum bias 0-86%, and at $\sqrt{s_{NN}}$ = 39 GeV in the minimum bias 0-86%.

measurements to direct photon p_T spectra (invariant yield) in the same centrality classes at both collision energies using the formula

$$\gamma^{\text{direct}} = (R_\gamma - 1)\ \gamma^{\text{hadron}}. \tag{3.1}$$

The calculated direct photon p_T spectra are shown in Fig. (5) and Fig. (6). In these plots one can also see the T_{AA}-scaled pQCD curves (from hard processes) based upon calculations from [6, 7],

where one of them is extrapolated down to $p_T = 1\,\mathrm{GeV/c}$ at the scale $\mu = 0.5\,p_T$. Note that $T_{AA} = N_{coll}/\sigma_{in}$.

In order to characterize the shape of the excess photon spectra at low-p_T observed in these figures, one can parametrize the data with a falling exponential function

$$\frac{1}{2\pi}\frac{d^2N}{dp_T dy} \sim \exp\left(-\frac{p_T}{T_{eff}}\right), \tag{3.2}$$

where the inverse slope parameter, T_{eff}, quantifies the shape of the spectra, however, cannot describe the temperature of the produced matter. We use Eq. (3.2) and extract the values of T_{eff} in the centrality classes under consideration. We fit this function with the direct photon data in the range of 0.5 GeV/c - 2.0 GeV/c.

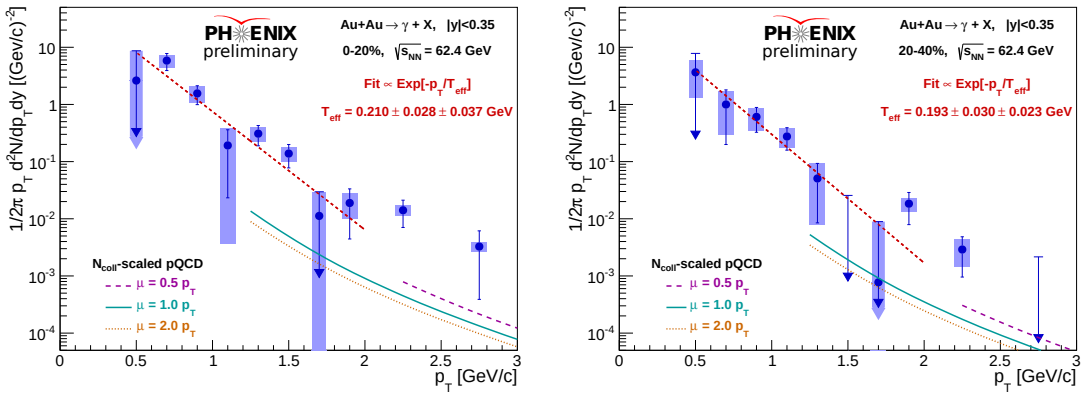

Figure 5: The invariant yield of direct photons at $\sqrt{s_{NN}}$ = 62.4 GeV in the centrality bins of 0-20% and 20-40%. The statistical errors are the vertical lines, the systematic errors are the boxes. The inverse slope T_{eff} is obtained from fitting with the data in the p_T range of 0.5 GeV/c - 2.0 GeV/c.

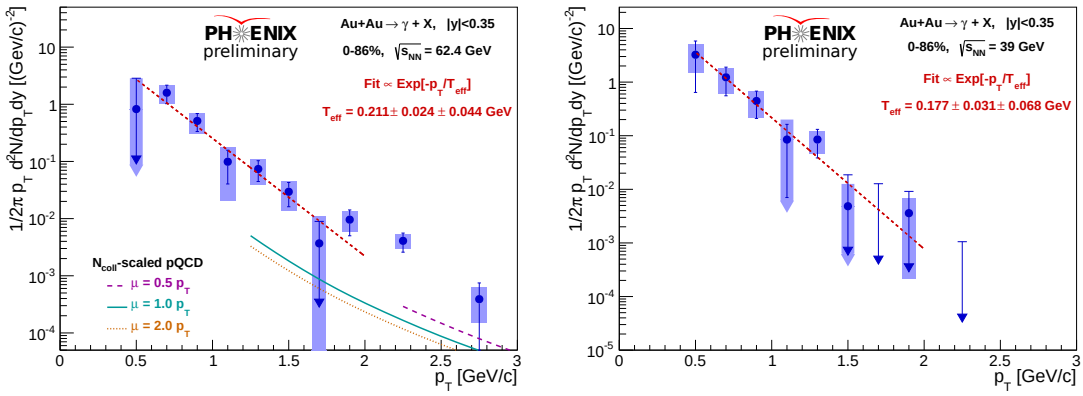

Figure 6: The invariant yield of direct photons at $\sqrt{s_{NN}}$ = 62.4 GeV in the minimum bias 0-86%, and at $\sqrt{s_{NN}}$ = 39 GeV in the minimum bias 0-86%. The inverse slope T_{eff} is obtained from fitting with the data in the p_T range of 0.5 GeV/c - 2.0 GeV/c.

Fig. 7 shows the obtained T_{eff} for the minimum bias systems at both $\sqrt{s_{NN}}$ = 62.4 GeV and $\sqrt{s_{NN}}$ = 39 GeV, and the comparison with the inverse slope from the PHENIX Au+Au (0-92%) at $\sqrt{s_{NN}}$ = 200 GeV and ALICE Pb+Pb (0-20%) at $\sqrt{s_{NN}}$ = 2760 GeV. However, we should point out that for our systems at lower beam energies, contrary to the systems at the other two energies, we obtain the values of T_{eff} without subtracting the contribution of the hard processes from the invariant yield. Other details are shown in Fig. 7.

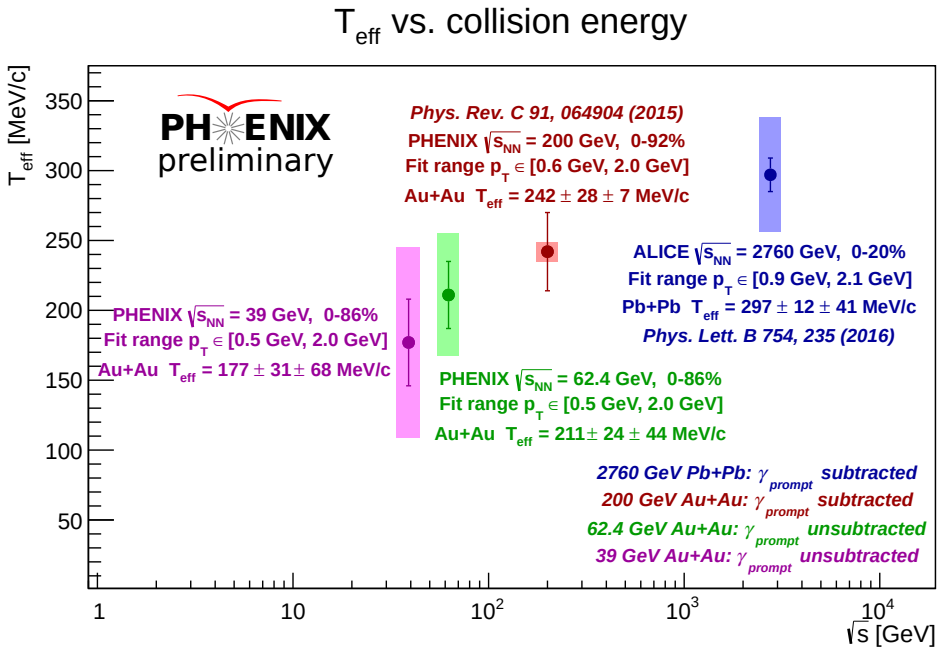

Figure 7: Data-extracted T_{eff} for four systems at four beam energies: 2760 GeV, 200 GeV, 62.4 GeV and 39 GeV.

4. The scaling of direct photons

One of the key observables to characterize the properties of the matter produced in relativistic heavy ion collisions is the multiplicity distribution of the charged-particle pseudorapidity density, $dN_{ch}/d\eta$, at midrapidity. We can have understanding on the relative contributions to particle production from hard and soft processes by investigating the dependence of the charged-particle multiplicity on the collision geometry, initial parton and energy densities of the produced matter. As the collision energy grows, the role of the hard processes also grow, which may provide insight into the partonic structure of the colliding nuclei.

PHENIX has measured the multiplicity distributions for a variety of collision systems from $\sqrt{s_{NN}}$ = 7.7 GeV to 200 GeV [8]. ALICE in turn has measured the distributions in Pb+Pb collisions at $\sqrt{s_{NN}}$ = 2.76 TeV and 5.02 TeV [9, 10]. PHENIX has also measured the midrapidity distributions of the transverse energy, $dE_T/d\eta$, along with $dN_{ch}/d\eta$. Some interesting findings show that the production of E_T and N_{ch} in collisions of symmetric nuclei depends on the collision energy and is independent of the size of the colliding system, nevertheless, one should also take into account

their dependence on the mean p_T of charged particles. The ratio of $dE_T/d\eta$ to $dN_{ch}/d\eta$ is found to be constant as a function of centrality for all collision systems and energies. Besides, a weak dependence of this ratio as a function of $\sqrt{s_{NN}}$ is observed too.

Since the direct photon spectra can be quantified by integrating the invariant yield above some p_T threshold value, one can also look at the surprising scaling properties of direct photons when we plot the low-p_T and high-p_T integrated yields vs. $dN_{ch}/d\eta$, as shown in Fig. (8) and Fig. (9).

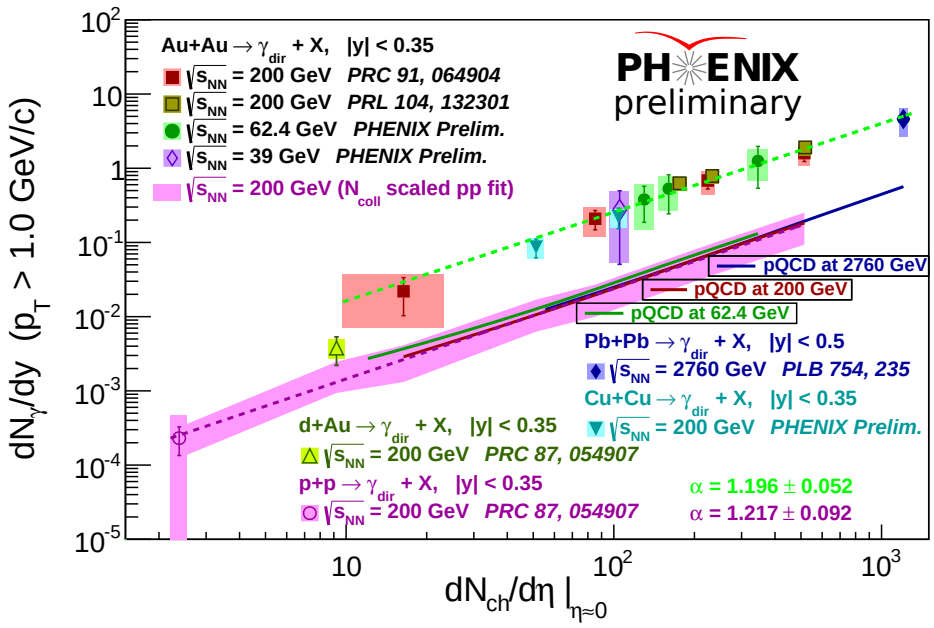

Figure 8: The direct photon integrated yield vs. charged-particle multiplicity for p_T integrated from 1.0 GeV/c, for five A+A datasets and one p+p dataset. The data in Au+Au are from [3], in Pb+Pb from [5], in Cu+Cu from [11], in d+Au from [12], and in p+p from [13]. The p+p fit describing the N_{coll} scaled prompt photons is obtained using a parameterization from [3]. Each model curve also describing these N_{coll} scaled prompt photons is the integrated prompt photon yield extrapolated down to $p_T = 1.0\,\mathrm{GeV}/c$, at respective beam energy. The extrapolated pQCD yield is from [7].

In these plots the direct photon data from heavy ions are fitted with the power-law function $(dN_{ch}/d\eta)^{\alpha}$. One can see that the integrated yield increases faster than the charged-particle multiplicity. An interesting feature is that the N_{coll} scaled prompt photons seem to have a similar scaling trend as that of heavy ion direct photons. One conclusion is that the underlying processes, which are responsible for the prompt photon production, can also be the source of direct photon production in heavy ion collisions. However, the ratio of their production rates reaches an order of magnitude.

References

[1] A. Adare *et al.* (PHENIX Collaboration), Phys. Rev. Lett. **104**, 132301 (2010) [arXiv:0804.4168 [nucl-ex]].

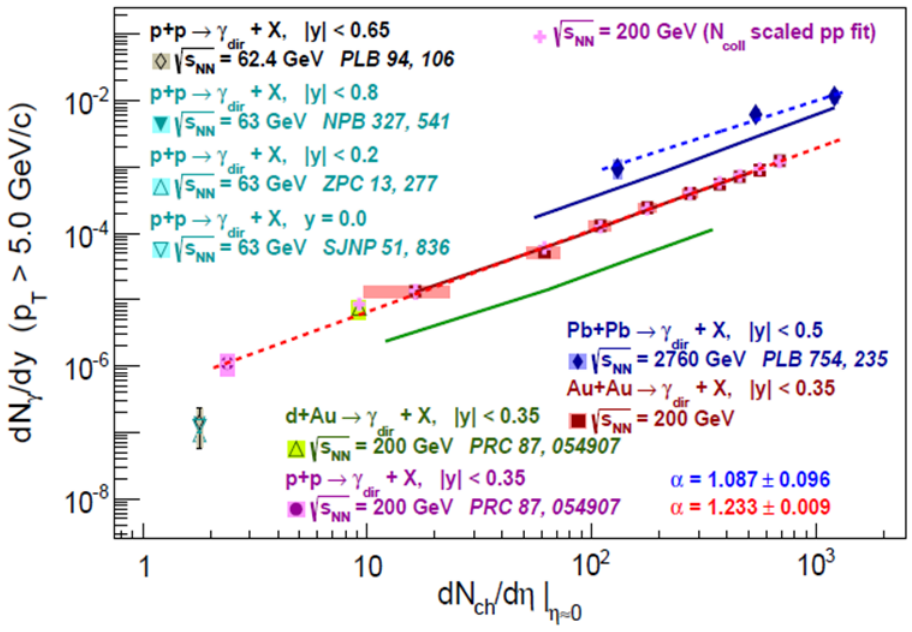

Figure 9: The direct photon integrated yield vs. charged-particle multiplicity for p_T integrated from 5.0 GeV/c, for two A+A datasets and five p+p datasets. The data in Pb+Pb are from [5], in Au+Au from [14], and in d+Au from [12]. The full p+p data points at 200 GeV are from [13], the other p+p data points at 62.4 GeV and 63 GeV are from [15]. The p+p fit has the same meaning as in the previous figure. Each pQCD curve is the integrated prompt photon yield at respective beam energy. The pQCD yield is from [7].

[2] A. Adare *et al.* (PHENIX Collaboration), Phys. Rev. C **81**, 034911 (2010) [arXiv:0912.0244 [nucl-ex]].

[3] A. Adare *et al.* (PHENIX Collaboration), Phys.Rev. C **91** 6, 064904 (2015) [arXiv:1405.3940[nucl-ex]].

[4] L. Adamczyk *et al.* (STAR Collaboration), Phys. Lett. B **770**, 451 (2017) [arXiv:1607.01447 [nucl-ex]].

[5] J. Adam *et al.* (ALICE Collaboration), Phys. Lett. B **754**, 235 (2016) [arXiv:1509.07324 [nucl-ex]]; M. Wilde *et al.* (ALICE Collaboration), Nucl. Phys. A **904-905**, 573 (2013) [arXiv:1210.5958 [hep-ex]].

[6] J.-F. Paquet, C. Shen, G. S. Denicol, M. Luzum, B. Schenke, S. Jeon and C. Gale, Phys. Rev. C **93**, 044906 (2016), [arXiv:1509.06738 [hep-ph]].

[7] J. F. Paquet, Private communication, (2017).

[8] A. Adare *et al.* (PHENIX Collaboration), Phys. Rev. C **93**, 024901 (2016).

[9] K. Aamodt *et al.* (ALICE Collaboration), Phys. Rev. Lett. **106**, 032301 (2011).

[10] J. Adam *et al.* (ALICE Collaboration), Phys. Rev. Lett. **116**, 222302 (2016).

[11] D. Sharma (for the PHENIX Collaboration), *PHENIX measurements of low momentum direct photons from large ion collisions as a function of beam energy and system size*, Quark Matter 2017.

[12] A. Adare *et al.* (PHENIX Collaboration), Phys. Rev. C **87**, 054907 (2013) [arXiv:1208.1234[hep-ex]].

[13] A. Adare *et al.* (PHENIX Collaboration), Phys. Rev. D **86**, 072008 (2012) [arXiv:1205.5533[hep-ex]].

[14] S. Afanasiev *et al.* (PHENIX Collaboration), Phys. Rev. Lett. **109**, 152302 (2012).

[15] W. Vogelsang and M. R. Whalley, J. Phys. G.: Nucl. Part. Phys. **23**, A1 (1997).